AIP | The Journal of Chemical Physics

Influence of shear on globule formation in dilute solutions of flexible polymers

Rangarajan Radhakrishnan and Patrick T. Underhill

Citation: The Journal of Chemical Physics **142**, 144901 (2015); doi: 10.1063/1.4917483
View online: http://dx.doi.org/10.1063/1.4917483
View Table of Contents: http://scitation.aip.org/content/aip/journal/jcp/142/14?ver=pdfcov
Published by the AIP Publishing

Influence of shear on globule formation in dilute solutions of flexible polymers

Rangarajan Radhakrishnan[1] and Patrick T. Underhill[2,a)]
[1]*Department of Physics, Durham University, Science Laboratories, South Road, Durham DH1 3LE, United Kingdom*
[2]*Department of Chemical and Biological Engineering, Rensselaer Polytechnic Institute, 110 8th Str., Troy, New York 12180, USA*

(Received 17 January 2015; accepted 2 April 2015; published online 13 April 2015)

Polyelectrolytes, polymers in poor solvents, polymers mixed with particles, and other systems with attractions and repulsions show formation of globules/structures in equilibrium or in flow. To study the flow behavior of such systems, we developed a simple coarse-grained model with short ranged attractions and repulsions. Polymers are represented as charged bead-spring chains and they interact with oppositely charged colloids. Neglecting hydrodynamic interactions, we study the formation of compact polymer structures called globules. Under certain conditions, increase in shear rate decreases the mean first passage time to form a globule. At other conditions, shear flow causes the globules to breakup, similar to the globule-stretch transition of polymers in poor solvents. © *2015 AIP Publishing LLC.* [http://dx.doi.org/10.1063/1.4917483]

I. INTRODUCTION

Many different systems containing polymers have attractive and repulsive interactions between the segments of a polymer. The balance between attractions and repulsions is typically varied by changing pH, temperature, and concentration of salt, proteins, or other charged particles.[1,2] Atomistic simulations of such systems are expensive due to the great difference between length and time scales of relaxation of long polymers and that of solvent-mediated interactions between its monomers. To permit the study of flow behavior of such systems, an implicit solvent Brownian dynamics (BD) simulation with effective interactions has been used previously.[3] This methodology is quite successful in modeling flow behavior of dilute polymer solutions with effective repulsive interactions between its segments.[4–6]

Although dilute solutions of flexible polymers with attractions are important for a number of different applications,[1,7,8] equilibrium behavior of these systems has received more attention than flow studies. Equilibrium behavior of dilute solutions of polymers in the presence of monovalent, multivalent salt, and dilute solutions of other particles has been investigated both theoretically and experimentally.[9–17] Until recently, few theoretical and experimental studies have been done to understand the interplay of attractive and repulsive interactions in determining their flow behavior.[3,7,8,18–28] Larson and Hoda[25] used a bead spring chain model of a polymer with bead-bead attractions and spring-spring repulsions, and they found the formation of shear-induced structures. Netz, Katz, and coworkers have used a bead spring chain model of a polymer with bead-bead interactions and studied the globule-stretch transition in shear and elongational flows.[7,20,22,27,28] However, these previous coarse-grained methods cannot capture flow-induced changes in polymer segment attractions that are mediated by particles, proteins, or salt ions. Recently, Chen *et al.* have performed Lattice Boltzmann simulations of polymers interacting with relatively large colloids in shear flow and found exciting results.[29–32] Particularly, for polymers having attractive interactions with colloids, they were able to observe the formation of reversible shear induced structures in both experiments and simulations.[31]

To capture the flow induced changes in the interactions between segments of a polymer, simulations of polymer beads interacting with co- and counter-ion beads in an implicit solvent can be used.[33–35] But, with this method it is computationally expensive to model long polymers in the presence of salt. In order to study flow behavior of long linear polymers interacting with nanoparticles, proteins, and other small molecules in a simple model, we have examined a dilute solution of polymer and colloids with attractions in the presence of salt. In contrast to previous work by Chen, Katz, and others,[29–32] we have examined the case where the radius of gyration of polymer is much larger compared to colloid size. The attractive interactions between segments of a polymer in a salt solution are mediated by oppositely charged colloids interacting via short ranged potentials. Neglecting hydrodynamic interactions between colloids and polymer, formation of compact structures of polymers and colloids called globules, and breakup of these globules are studied in equilibrium and in shear flow. We expect the role of hydrodynamic interactions to affect the quantitative results, but the features exhibited by the simpler model in this study can be used to guide future work. Recently, we have used the model developed in this article and found interesting stress versus strain response due to hopping between the different states of the system in large amplitude oscillatory shear.[36] This article examines the formation and dynamics of such states in steady shear flow.

a)Author to whom correspondence should be addressed. Electronic mail: underhill@rpi.edu

II. MODEL AND SIMULATION METHODOLOGY

A. Model

The polymer is modeled as a bead spring chain connected by finitely extensible (FENE) springs, whose force is given by

$$F_s(Q) = \frac{3k_BTQ}{R_H^2(1-(\frac{Q}{Q_0})^2)}, \tag{1}$$

where k_B is the Boltzmann's constant, T is the temperature, $R_H^2 = N_{K,s}l^2$ is the size of a Hookean spring (linear spring) in theta conditions, $N_{K,s}$ is the number of Kuhn steps per spring, l is the Kuhn length, Q is the extension of the spring, and $Q_0 = N_{K,s}l$ is the maximum length of the spring. The polymer interacts with colloid beads in a large simulation box. The colloid and polymer beads are oppositely charged and interact by means of short ranged Debye-Huckel (DH) potential U_{DH} given by

$$U_{DH}(r_{ij}) = \frac{-A^*k_BTR_H}{r_{ij}}\exp(-\kappa^*\frac{r_{ij}}{R_H}), \tag{2}$$

where $A^*k_BTR_H = |q_iq_j|/(4\pi\epsilon_0\epsilon_r)$ determines the strength of interaction between beads i and j with charges q_i and q_j in a material with dielectric constant ϵ_r and the permittivity of vacuum ϵ_0, r_{ij} is the separation between the beads, and $\kappa^* = \kappa R_H$ determines the range of interaction, where κ^{-1} is the Debye length. The Weeks-Chandler-Anderson (WCA) potential[37] is used to prevent the overlap of colloid and polymer beads, and is given by

$$U_{WCA}(r_{ij}) = \begin{cases} 4\epsilon\left[\left(\frac{\sigma}{r_{ij}}\right)^{12} - \left(\frac{\sigma}{r_{ij}}\right)^{6}\right] + \epsilon, & r_{ij} < 2^{1/6}\sigma \\ 0, & r_{ij} \geq 2^{1/6}\sigma \end{cases}, \tag{3}$$

where ϵ determines the strength of interaction and σ determines the range of interaction. Although Debye-Huckel potential is a very good approximation only up to 0.01M of monovalent salt,[38] we use it to capture the key features of a short-ranged interaction, which are the energy and the range of interaction. We expect any other short-ranged potential with the same interaction energy and range will exhibit the same qualitative features as observed in this article. Note that for the small Debye lengths used here, the shear flow will not be strong enough to distort the counter-ion clouds and alter the Debye-Huckel potential.

B. Simulation methodology

We use BD simulations to follow the time evolution of our model, similar to many earlier studies of polymers and colloids.[3–6,39,40] In BD simulations, the particles obey Newton's laws of motion in an implicit solvent. The force balance on any particle is given by

$$m\ddot{\mathbf{r}} = \mathbf{F_s} + \mathbf{F_d} + \mathbf{F_B}, \tag{4}$$

where $\mathbf{F_B}$ is a Brownian force, $\mathbf{F_s}$ are the systematic forces (which includes external and spring forces), and $\mathbf{F_d}$ is the force due to drag. Neglecting the acceleration term and tracking the motion of a particle at time scales larger than the inertial time scale, only the balance of other forces is considered,

$$0 \approxeq \mathbf{F_s} + \mathbf{F_d} + \mathbf{F_B}. \tag{5}$$

In the Stokes' limit at very low Reynolds number, the drag force on a particle at a distance $\mathbf{r}$ from the origin, without considering hydrodynamic interaction from other particles, is given by

$$\mathbf{F_d} = -\zeta\left(\mathbf{v_p} - \mathbf{v_s}(\mathbf{r})\right), \tag{6}$$

where $\mathbf{v_p} = \dot{\mathbf{r}}$ is the velocity of the particle, $\mathbf{v_s}(\mathbf{r})$ is the velocity of the undisturbed solvent at that particle's position, and ζ is the drag coefficient of the particle. The random Brownian force $\mathbf{F_B}$ should satisfy the fluctuation dissipation theorem.[40] Therefore, the Brownian force satisfies $\langle\mathbf{F_B}(t)\cdot\mathbf{F_B}(s)\rangle = 2k_BT\zeta\delta(t-s)$ and $\langle\mathbf{F_B}\rangle = 0$. Equation (5) is integrated by stepping forward in time by a first order Euler-Maruyama scheme of integration.[40]

A dilute solution of a polymer and colloids was simulated in a box of dimensions $L_{box}\times W_{box}\times W_{box}$ containing a single bead-spring chain and N_{col} colloids. The motion of all the beads was computed by means of BD simulations. Periodic boundary conditions were applied in equilibrium and in non-gradient directions in shear flow. In the gradient direction of shear, Lees-Edwards boundary conditions were applied.[35,41] The simulation box was taken such that in the flow direction $L_{box} \geq N_Kl$, and in the gradient and neutral directions $W_{box} \geq 2R_{g,\theta}$, where $R_{g,\theta}$ is the theta solvent radius of gyration of the polymer. To eliminate any bias due to use of periodic boundary conditions in the flow direction, care was taken to ensure that L_{box} was long enough that the diffusion time for particles to move across the width $t_D = \zeta W_{box}^2/(2k_BT)$ was less than the time scale specified by maximum velocity of the particle $t_v = 2L/(\dot{\gamma}W_{box})$.

C. Choice of simulation parameters

The bead-spring chain was chosen to represent a long flexible polymer such as sodium polystyrene sulfonate (NaPSS), which had been previously parameterized into a bead spring chain model by Pamies *et al.*[42,43] NaPSS of molecular weight of $M_W \approx 3\times10^5$ g/mol, has number of Kuhn steps $N_K \approx 81$. The choice of number of beads $N = 10$ of a chain was made such that the bead-spring chain has sufficient flexibility and also making sure that number of Kuhn steps per FENE spring ($N_{K,s} = 9$) is reasonable to represent the force extension of such a molecule correctly.[44] A dilute colloid concentration was chosen, with $N_{col} = 200$ colloids in a volume $V = (N_Kl)^3$ which corresponds to a colloid volume fraction of 4.26×10^{-5}. Other parameters in the simulations were $\sigma = 0.1R_H$, and $\epsilon = k_BT/12$. The diffusivities of the colloids were varied by changing the drag coefficients of the colloids $\zeta_c = \zeta_0\zeta_c^*$, where ζ_0 is a constant and is equal to the polymer bead drag coefficient ζ_p. While the colloid and polymer beads are both given the same excluded volume size σ, the drag coefficient of the colloids is changed independently simply as a way of understanding the mechanism by varying the colloid diffusion. A^* and κ^* of U_{DH} were varied between the range $1-10$, similar to previous works.[42,43] For simplicity, we kept A^* and κ^* the same for both colloid-polymer bead attractions and bead-bead repulsions, except for the reversal in sign. Therefore, two polymer beads or two colloid beads interact with the repulsion

version of Eq. (2) while one polymer bead and one colloid bead interact with the attractive version of Eq. (2).

Compact structures of polymer and colloids were formed in our simulations, which we call "globules." A globule is defined as the state of the polymer when the radius of gyration R_g satisfies $R_g < 0.37R_{g,\theta}$, where $R_{g,\theta}$ is the average radius of gyration of the polymer in theta conditions. The probability of this occurring without the colloids is very small. A theoretical expression for probability of R_g in a theta solvent is given by[45]

$$P(R_g^2) = 18\left(\frac{6}{\pi\langle R_g^2\rangle}\right)^{1/2} t^{-5/2} \exp\left(-\frac{9}{4t}\right), \tag{7}$$

where

$$t = \frac{R_g^2}{\langle R_{g,\theta}^2\rangle} = \frac{6R_g^2}{N_K l^2}. \tag{8}$$

Using the above expression, we find that $P(R_g < 0.37R_{g,\theta}) \sim O(10^{-6})$. It was verified that lowering this criterion ($P(R_g < 0.32R_{g,\theta}) \sim O(10^{-8})$) does not affect the qualitative features of the results presented in this article. All of the simulations were started from an initial random coiled state of the polymer and random positions of the colloids, unless specified otherwise. From such a random state, the time taken by a molecule to form a globule is called the first passage time of globule formation. At least 40 independent simulations were used to calculate mean first passage time (MFPT) (M_t) of globule formation. We also performed equilibrium simulation of the polymer colloid system to test our theories. All of the simulations were performed up to a minimum of $200\lambda_\theta$, where $\lambda_\theta = 1.7\zeta_p R_H^2/(k_BT)$ is the longest relaxation time of a 10 bead chain connected with Hookean springs in a theta solvent.[46] The strength of the shear flow is quantified using the Weissenberg number with this relaxation time as $Wi = \dot{\gamma}\lambda_\theta$.

We can compare our model system against a number of experimental systems to illustrate the wide prevalence of such systems. Estimates of κ^* for different polymers of $N_K = 81$ in 10 mM NaCl solution are shown below. ds-DNA has a $\kappa^* \sim 150$ assuming Kuhn length $l \sim 100$ nm and Debye length $\kappa^{-1} \sim 2$ nm;[6,47] ss-DNA has a Kuhn length $\kappa^{-1} \sim l$,[48] which implies $\kappa^* \sim 3$; and NaPSS with molecular weight of $M_w \approx 3 \times 10^5$ g/mol and assuming $l = 4.6$ nm has $\kappa^* \sim 7$.[42,43] To obtain the interaction energy A^*, the charge on the polymer is assumed to be distributed along the beads of the model with a degree of ionization due to counterion condensation,[42,43] which could be obtained from reported values from the literature. Assuming Bjerrum length $l_B = 0.714$ nm, for ds-DNA with charge separation of 0.17 nm, 24% ionization[49] gives $A^* \sim 3 \times 10^3$. The large Kuhn length for ds-DNA leads to a large charge assigned to each bead, and therefore a large A^*. Assuming charge separation of 0.4 nm and 66% ionization[48] for ss-DNA gives $A^* \sim 85$. For NaPSS, assuming charge separation of 0.3 nm and 10% ionization[42,43] gives $A^* \sim 8$. For the colloid-polymer interaction to have the same A^*, we can calculate the potential for the colloids using $q/(4\pi\epsilon_0\epsilon_r\sigma)$ which does not include any counter-ion condensation. Assuming colloids of size $\sigma = 0.1R_H$ gives the surface charge potential of the colloids as 0.7 V for ds-DNA, 0.8 V for ss-DNA, and 0.16 V for NaPSS systems.

Another method for comparing the model with experimental systems is to compare the binding energy of the polymers with colloids or proteins. The parameters A^*, κ^* can be chosen to match the overall binding free energy of the polymer and colloid/protein under consideration. The non-specific binding of ds-DNA to proteins or colloids has approximate free energies of $\sim O(10)k_BT$[50,51] and the binding energy of 16 base pair ds-DNA with poly-L-lysine was recently estimated from an MD simulation to be ~50–100 k_BT.[52] The binding energy of Laponite clay with poly(ethylene oxide) (PEO) is a few k_BT.[53] Binding energy E_B of colloids to the polymer beads in our simulations is obtained by calculating the minimum of the potential energy between a polymer bead and a colloid, $E_B = U_{WCA}(\delta_m) + U_{DH}(\delta_m)$, where δ_m is the distance at which $U_{WCA} + U_{DH}$ is minimum. For the simulations presented here, the binding energies of the colloids to the polymers are comparable to these experimental systems.

III. RESULTS AND DISCUSSION

A large number of experimental systems, such as dilute solutions of polyelectrolytes,[14,54,55] polymers in poor solvents,[56,57] polymers mixed with particles,[1,15] and other systems with attractions and repulsions,[58,59] show formation of compact structures in equilibrium or in flow. Similar to some of the experimental systems, we find that a simple system of particles and polymers with attractions can show globule formation. Before we can study the flow behavior of such a system, we need to have an understanding of the conditions required for globule formation in equilibrium. Specifically, we are interested in the range of interaction parameters κ^* and A^* that can show globule formation, for a given WCA potential, and concentration of polymer and colloids.

A. Globule formation in equilibrium

Globule formation in polymer solutions at equilibrium can be understood by a free energy balance theory.[9,11–13,60,61] Using ideas similar to previous studies but applied to our system, a free energy model can be developed for our polymer/colloid mixture. As illustrated in Fig. 1, we approximate colloids as either free or bound to a polymer bead, and each polymer bead can either have zero attached colloids (denoted m) or one attached colloid (denoted m^*). Considering only two body interactions, globule formation can be explained from the balance between enthalpy of attachment of colloids compared to the entropy of colloids and polymer. Note that higher order terms can be invoked to model the equilibrium states more precisely. These terms would be necessary to keep the globule

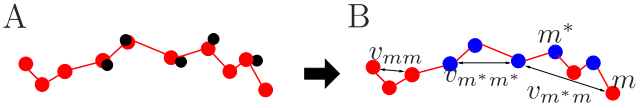

FIG. 1. Theoretical representation of a polymer interacting with colloids. (a) Polymer with $N_C = 5$ attached colloids. (b) Theoretical representation of the polymer model in (A), where the effective two body interactions between beads with bound colloids (m^*) and free beads (m) are given by v_{mm}, $v_{m^*m^*}$, and v_{m^*m}.

state from collapsing, but the focus here is to understand the formation of globules from the coil state. The total free energy of the system F_{sys} in a volume V in this theory is given by

$$\begin{aligned}\frac{F_{sys}}{k_BT} &= \frac{X}{R_g^2} + YR_g^2 + p(N-N_c)(N-1-N_c)\frac{v_{mm}}{R_g^3} \\ &+ pN_c(N_c-1)\frac{v_{m^*m^*}}{R_g^3} + 2pN_c\,(N-N_c)\,\frac{v_{m^*m}}{R_g^3} \\ &+ (N_{col}-N_c)\,(\ln(v_{rat}(N_{col}-N_c))-1) \\ &- \ln\frac{N!}{(N-N_c)!\times N_c!} - \frac{N_cE_B}{k_BT}, \end{aligned} \tag{9}$$

where X and Y are the constants determining the free energy change due to entropy of the polymer, N_c is the number of polymer beads with attached colloids, v_{rat} is the ratio of the volume of a colloid to that of the simulation box, E_B is the energy of adsorption of a colloid, and p is the prefactor to the interaction energy terms. The three possibilities for two body interaction terms between beads along the polymer chain are given by the terms v_{mm}, v_{m^*m}, and $v_{m^*m^*}$.

The first two terms of the equation determine the entropy of the polymer without repulsions, and therefore the factors X and Y can be fit using simulations with $A^* = 0$. The free energy contribution by polymer bead repulsions is given by the third term. Free energy due to attractions between polymer beads with attached colloids (m^*) and those without attached colloids (m) is given by the fourth and fifth terms. Note that for the parameters used here, both of these terms give effective attractions where a colloid bridges two polymer beads. For small A^* and/or large Debye lengths, it is possible for these to give net repulsions but those would not correspond to cases that form globules. Assuming non-interacting colloids, the free energy due to the entropy of colloids is given by the sixth term.[13,62] The seventh term quantifies the entropy due to different configurations available for a polymer with N_c attached colloids. Note that, unlike the sixth term, we have not used the Sterling approximation[62] for the factorials. The final (eighth) term is the free energy due to colloid binding, where E_B can be estimated as stated in Sec. II.

In principle, the factor p is different among the three terms, but we assume them to be equal for simplicity. The value of p is calculated by matching the 3rd term with BD simulations with $N_{col} = 0$. Based on the attractive and repulsive potentials, v_{mm}, v_{m^*m}, and $v_{m^*m^*}$ can be computed as shown in the supplementary material.[63]

A surface plot of the free energy as shown in Fig. 2 is useful in visualizing the implications of Eq. (9). Fig 2(a) shows the free energy of a system F_{sys} that has a metastable state (denoted state I). F_{sys} decreases with increase in the number of attached colloids N_C; there is a compact globule state that is favored at very small R_g (denoted state II) and also a non-compact metastable state with attached colloids at a higher R_g, with an energy barrier between the two states. The saddle point between the two states is denoted by state III. This indicates the possibility of hopping transitions between globule and non-globule states of the system. An energy barrier in the free energy diagram can be used as a criterion for globule formation of polymers at equilibrium. Comparing the free energy gain change to the loss of entropy of a colloid to the enthalpic

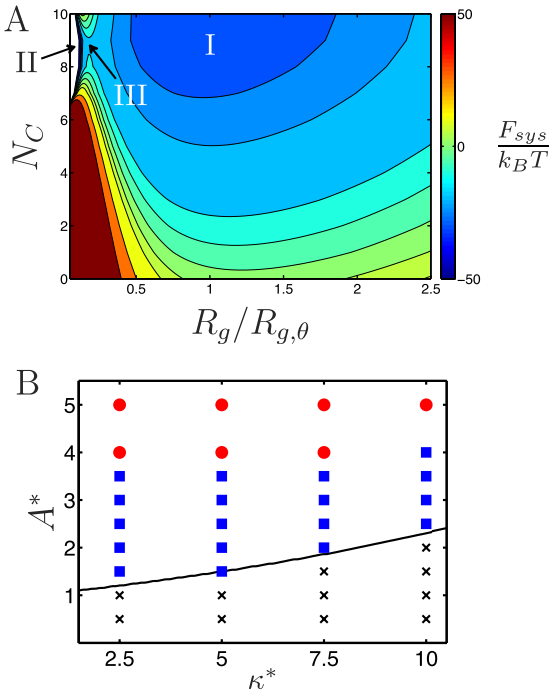

FIG. 2. (a) Free energy landscape calculated from Eq. (9) with $A^* = 1.5$ and $\kappa^* = 2.5$ for the polymer-colloid system. It shows the existence of a metastable state which is not a globule (state I). State II has a large negative free energy, with the white region having a free energy less than −50 and which is beyond the color-bar. State III is the saddle point between the other two states. (b) Phase diagram of globule formation at equilibrium of the polymer-colloid system. The polymer can exist in the coiled (×), globule (•), or hop between the globule and the coiled states (■). The solid black line is the phase boundary between the coiled and the other states given by the globule formation criterion Eq. (10).

gain of attachment of a colloid (i.e., does F_{sys} decreases as N_C increases from zero) allows an estimate of a criterion for globule formation, which is given as

$$|\ln(v_{rat}N_{col})| \lesssim E_B/(k_BT). \tag{10}$$

This criterion quantifies whether it is favorable for colloids to attach on the polymer chain. Since polymer beads are repulsive with each other, attachment of colloids to polymer beads is a necessary condition for globule formation. It need not be a sufficient condition, since interaction parameters determine the existence of a globule state versus a coiled polymer with colloids condensed on the backbone. Equation (10) serves as an estimate to check the validity of the theory for the results from BD simulations at equilibrium.

Figure 2(b) shows good agreement between this criterion and with simulations on a phase-plot of the strength and range of interactions. The results show a range of parameters for which the polymer remains in the coiled state, globule state, or hops between the two states. To determine the states of the polymer-colloid system, BD simulations with initial configurations in coiled and globule states were performed. Systems in the coiled state are those which never form a globule from the random coil state and returning to the random coil state if the initial configuration was a globule. Systems in the globule state form globules and never leave the globule state. Systems that are said to "hop" form globules from a random coil state and vice-versa. The phase-boundary for

globule formation given by the criterion for globule formation separates the coiled states from those that attain the globule state at least once. This figure also illustrates the sensitivity of the free energy to the interaction parameters. If the free energy favors the coiled or globule states, it is less sensitive to the interaction parameters. However, on the boundaries of those regions, and when the system can hop between the states, the free energy landscape can be very sensitive to the interaction parameters.

A simple criterion for separating the hopping states from the globule states cannot be obtained from the current theory as higher order interaction terms in Eq. (9) were not considered. Inclusion of three body interaction terms in Eq. (9) is needed to prevent divergence of F_{sys} at low R_g and predict the free energy landscape near the globule state more accurately, but it is quite difficult to find explicit analytical solutions for these parameters. This divergence in free energy is state II in Fig. 2(a) which is the white region with free energy below −50 which is beyond the color-bar. Numerical fits to three body terms could be obtained for individual systems but are not pursued in this article.

It is interesting to note the differences between the model proposed in this article with the case of counterion condensation on a polyelectrolyte by Muthukumar.[13] If the monovalent salt condenses on the polymer backbone or colloids, that would act to reduce the interaction parameter A^*. But we can also view the colloids as counter-macroions which are considered explicitly (as opposed to the monovalent salt which is treated implicitly). Since the model considers a dilute solution of colloids, fluctuations due to colloid-colloid interaction are neglected in Eq. (9). Fluctuations between uncondensed counterions and co-ions are determined by salt concentration in the solution and are not captured in our model. Another aspect not explicitly considered in our model is the interaction of a polymer with its surrounding counter-ion cloud which is important in some systems and would lead to globule formation without colloids, but is not expected to play an important role here.

B. Impact of shear flow on globule formation and breakup

The main advantage of and goal of using the coarse-grained model developed in this article is to study flow behavior. Since the microscopic structure can determine dynamic properties such as viscosity and stress, the impact of simple shear flow on formation and breakup of globules is studied.

Although the globule state can be a global minimum free energy state, the time for globule formation depends on its kinetics. Therefore, the MFPT of globule formation in shear flow was studied for a system that satisfies the globule formation criterion. BD simulations of polymer-colloid systems having strong interactions with $A^* = 10$, $\kappa^* = 10$ were considered for our analysis. Systems with strong interactions form globules faster compared to systems with weaker interactions, and allow shorter computation times for MFPT. It was found that there is a decrease in the MFPT $\sim \dot{\gamma}^{-1/2}$ as shear rate is increased for systems with strong

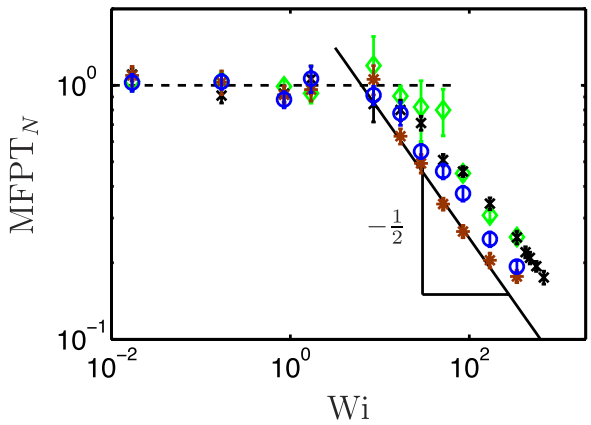

FIG. 3. Decrease in MFPT_N of globule formation of a polymer with strong attractions under shear as a function of the Weissenberg number. Polymer-colloid systems of $A^* = 10$, $\kappa^* = 10$ with different colloid drag coefficients $\zeta_c^* = 0.5$ (◇), $\zeta_c^* = 1$ (×), $\zeta_c^* = 2$ (○), and $\zeta_c^* = 4$ (∗) are shown.

interactions as shown in Fig. 3. A previous BD simulation study of semiflexible polymers has shown a similar increase in the rate of formation of compact structures with increase in shear rate.[64] For comparison of polymer-colloid systems with different diffusivities, the MFPT was normalized using the low shear rate values of MFPT to give a normalized-MFPT (MFPT_N). The systems with larger colloid drag coefficient produce a larger un-normalized MFPT because it takes the colloids a longer time to find the polymer (data not shown). The decrease in MFPT_N with increase in $\dot{\gamma}$ indicates that the globules are formed faster in shear. The decrease occurs for $\mathrm{Wi} > 1$ when the polymer undergoes tumbling and is stretched by flow. The flux of particles reaching the polymer scales as a typical relative velocity times the cross-sectional area of the polymer. The typical relative velocity is $\dot{\gamma}$ times the width of the polymer in the gradient direction δ. Therefore, the MFPT should scale as $\sim 1/(\dot{\gamma}\langle\delta^2\rangle)$. Since for a polymer chain without HI, $\langle\delta^2\rangle \sim \dot{\gamma}^{-1/2}$,[65,66] we have the required scaling for MFPT. Increase in drag coefficients ζ_c^* decreases the combined diffusivity of attached colloid and polymer bead, thereby decreasing the prefactor to MFPT_N scaling as seen in Fig. 3.

For $\mathrm{Wi} > 1$ in shear flow, the probability of compact states ($R_g < 1$) for a polymer without colloids decreases with increase in shear rates even for a polymer with $A^* = 0$, as shown in the supplementary material.[63] It also indicates that decrease in polymer size observed in this article is not related to ultra-high shear rate ($\mathrm{Wi} > N_K^2$) compaction of the polymer chain studied by Sendner and Netz,[67] and later elucidated by Dalal *et al.*[66] Further evidence pointing to attachment of colloids in stretched polymers leading to globule formation by the mechanism described above is that the MFPT is inversely proportional to colloid concentration as shown in the supplementary material.[63]

The breakup of globules in shear flow has received much attention recently due to its importance in biology and in determining properties of gels.[28] Even though shear decreases MFPT of globule formation, we expect high shear rates to overcome strong attractions and stretch the globule. It has been observed that polymers in poor solvents undergo a globule to stretch transition at a critical strain rate and that the stretching

of the molecule is suppressed when the attractions between polymer segments are increased.[28]

Systems with strong interactions, such as those shown in Fig. 3, stay in globule states until very high shear rates. In order to see the globule-stretch transition at smaller shear rates, we simulated systems which show hopping transitions between coil and globule state even in equilibrium, with the initial configuration of the system in the globule state. The size of the polymer $\langle R^2 \rangle$ in shear flow from the BD simulations is shown in Fig. 4(a). Below a critical shear rate $\dot{\gamma}_c$, the $\langle R^2 \rangle$ is a constant and the $\langle R^2 \rangle$ of polymer increases as the strength of interactions A^* is decreased at a constant κ^*. Above $\dot{\gamma}_c$ the globules "breakup" and undergo hopping transitions from the globule to the stretched states as shown in Fig. 4(b). The peaks in R^2 are similar between the different systems, meaning that these systems behave similarly once in a stretched state. However, systems with higher A^* have a higher strength of interaction and spend a longer time in the globule state. Future studies will quantify in detail the statistics of the transitions between the two states including how they depend on the interactions between the polymer and colloids and on the shear rate. At high shear rates, all of the polymers undergo similar dynamics as that of the polymer in theta solvent. The high shear rate response appears to be in contrast to the model of hydrophobic polyelectrolytes by Larson and Hoda,[25] which remains in the globule state.

The shear flow response is similar to a system with polymer segment attractions.[28] An important difference between

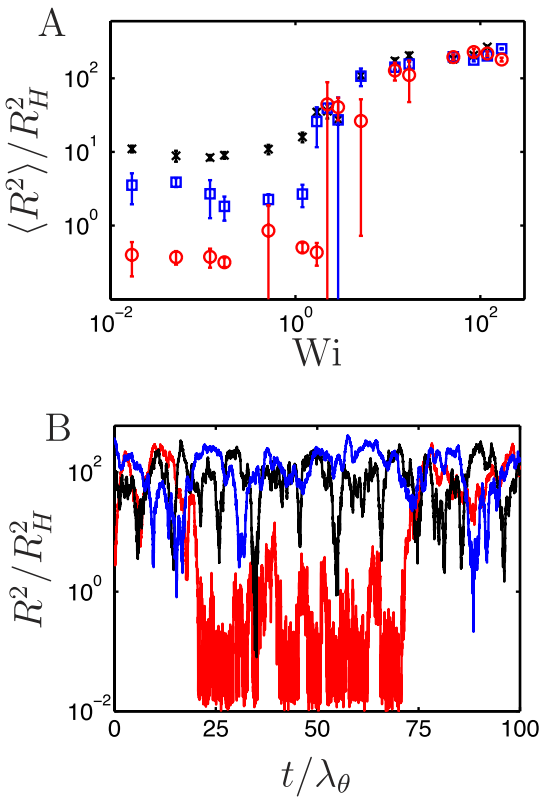

FIG. 4. Breakup of globules in shear flow of systems with $\kappa^* = 10$, and $A^* = 2.5$ (black), $A^* = 3$ (blue), and $A^* = 3.5$ (red). (a) The average size of the polymers in steady shear as a function of the Weissenberg number. (b) The time dynamics of these polymers at $\dot{\gamma}\lambda_\theta = 5.1$. Systems with increasing strengths of interactions spend longer time in the globule state.

our system and that of Sing and Alexander-Katz[28] undergoing globule-stretch transitions is that the colloids can detach from the polymer beads in shear flow. Our model shows a monotonic increase of the average polymer size with increasing shear rate, while a decrease in $\langle R^2 \rangle$ with increase in $\dot{\gamma}$ was observed using the model with polymer segment attractions[28]. Sing and Alexander-Katz[28] attribute this decrease in $\langle R^2 \rangle$, even in theta conditions, to the inclusion of HI between beads of the polymer. Since bead-bead HI was neglected in our model, there is no significant decrease in $\langle R^2 \rangle$ for different parameters that we had simulated.

IV. CONCLUSIONS

A framework for understanding the response in flow of polymer-colloid systems with different sizes and interactions in a computationally feasible model is presented in this article. A simple bead-spring chain model of a polymer interacting with oppositely charged colloids with short-ranged potentials is used. A simple equilibrium free energy landscape theory for our model system was derived similar to previous studies[9,11–13,60,61] in order to predict and understand equilibrium formation of compact polymer-colloid structures called globules. A simple criterion for globule formation from such a theory matches well with equilibrium BD simulations for different interaction parameters. Shear flow simulations of a system with strong attractions show that globules are formed faster in flow. This is surprising because flow typically stretches polymers. We determined that the decrease in globule formation time was due to a combination of the advection of the colloids by the flow and the stretching and tumbling of the polymer.

The globules that form can be broken (undergoing a globule-stretch transition) if the flow is strong enough. This transition was investigated for systems with moderate interactions between the polymer and colloids. Such a transition had not been seen previously in a system made of a mixture of polymers and colloids. Future experiments of systems with nanoparticles and polymers are needed to verify the conclusions of the simulations presented in this work. In future work, the simulations will be used to quantify the interesting polymer fluctuations at the globule-stretch transition. The free energy model used here has been used in similar forms for a wide range of polyelectrolyte systems at equilibrium. This suggests that the work here could also be extended to examine the flow behavior of related phenomena including compaction of polymers by multivalent ions (the colloids act similarly to the ions) or complex coacervation.

ACKNOWLEDGMENTS

We gratefully acknowledge support by NSF Grant No. CBET-0954445.

[1]A. Estevez-Torres and D. Baigl, Soft Matter **7**, 6746 (2011).
[2]M. Doi and S. F. Edwards, *The Theory of Polymer Dynamics* (Oxford University Press, New York, 1988).
[3]R. G. Larson, J. Rheol. **49**, 1 (2005).
[4]C. M. Schroeder, E. S. G. Shaqfeh, and S. Chu, Macromolecules **37**, 9242 (2004).

[5]C. M. Schroeder, R. E. Teixeira, E. S. G. Shaqfeh, and S. Chu, Macromolecules **38**, 1967 (2005).
[6]E. S. G. Shaqfeh, J. Non-Newtonian Fluid Mech. **130**, 1 (2005).
[7]A. Alexander-Katz, M. F. Schneider, S. W. Schneider, A. Wixforth, and R. R. Netz, Phys. Rev. Lett. **97**, 138101 (2006).
[8]I. B. Bekard, P. Asimakis, J. Bertolini, and D. E. Dunstan, Biopolymers **95**, 733 (2011).
[9]M. O. de la Cruz, L. Belloni, M. Delsanti, J. P. Dalbiez, O. Spalla, and M. Drifford, J. Chem. Phys. **103**, 5781 (1995).
[10]M. J. Stevens and K. Kremer, Phys. Rev. Lett. **71**, 2228 (1993).
[11]E. Raspaud, M. O. de la Cruz, J.-L. Sikorav, and F. Livolant, Biophys. J. **74**, 381 (1998).
[12]H. Schiessel and P. Pincus, Macromolecules **31**, 7953 (1998).
[13]M. Muthukumar, J. Chem. Phys. **120**, 9343 (2004).
[14]A. V. Dobrynin and M. Rubinstein, Prog. Polym. Sci. **30**, 1049 (2005).
[15]A. A. Zinchenko, K. Yoshikawa, and D. Baigl, Phys. Rev. Lett. **95**, 228101 (2005).
[16]H. Boroudjerdi, A. Naji, and R. R. Netz, Eur. Phys. J. E **34**, 1 (2011).
[17]J.-M. Y. Carrillo and A. V. Dobrynin, Macromolecules **44**, 5798 (2011).
[18]Y. Otsubo, Langmuir **8**, 2336 (1992).
[19]J. Wang, R. Bai, and D. D. Joseph, J. Fluid Mech. **516**, 335 (2004).
[20]S. W. Schneider, S. Nuschele, A. Wixforth, C. Gorzelanny, A. Alexander-Katz, R. R. Netz, and M. F. Schneider, Proc. Natl. Acad. Sci. U.S.A. **104**, 7899 (2007).
[21]P. Szymczak and M. Cieplak, J. Chem. Phys. **127**, 155106 (2007).
[22]A. Alexander-Katz and R. R. Netz, Macromolecules **41**, 3363 (2008).
[23]M. Kamibayashi, H. Ogura, and Y. Otsubo, J. Colloid Interface Sci. **321**, 294 (2008).
[24]X. Zhang, K. Halvorsen, C.-Z. Zhang, W. P. Wong, and T. A. Springer, Science **324**, 1330 (2009).
[25]N. Hoda and R. G. Larson, J. Rheol. **54**, 1061 (2010).
[26]N. Y. Chan, M. Chen, X.-T. Hao, T. A. Smith, and D. E. Dunstan, J. Phys. Chem. Lett. **1**, 1912 (2010).
[27]C. E. Sing and A. Alexander-Katz, Macromolecules **43**, 3532 (2010).
[28]C. E. Sing and A. Alexander-Katz, Phys. Rev. Lett. **107**, 198302 (2011).
[29]H. Chen and A. Alexander-Katz, Soft Matter **9**, 10381 (2013).
[30]H. Chen and A. Alexander-Katz, Phys. Rev. Lett. **107**, 128301 (2011).
[31]H. Chen, M. A. Fallah, V. Huck, J. I. Angerer, A. J. Reininger, S. W. Schneider, M. F. Schneider, and A. Alexander-Katz, Nat. Commun. **4**, 1333 (2013).
[32]H. Chen and A. Alexander-Katz, Phys. Rev. E **89**, 032602 (2014).
[33]R. Chang and A. Yethiraj, J. Chem. Phys. **116**, 5284 (2002).
[34]T. Zhou and S. B. Chen, J. Chem. Phys. **124**, 034904 (2006).
[35]C. Stoltz, J. J. de Pablo, and M. D. Graham, J. Chem. Phys. **126**, 124906 (2007).
[36]R. Radhakrishnan and P. T. Underhill, AIChE J. **60**, 1365 (2014).
[37]J. D. Weeks, D. Chandler, and H. C. Andersen, J. Chem. Phys. **54**, 5237 (1971).
[38]K. S. Pitzer, Acc. Chem. Res. **10**, 371 (1977).
[39]D. L. Ermak and J. A. McCammon, J. Chem. Phys. **69**, 1352 (1978).
[40]P. S. Grassia, E. J. Hinch, and L. C. Nitsche, J. Fluid Mech. **282**, 373 (1995).
[41]A. W. Lees and S. F. Edwards, J. Phys. C: Solid State Phys. **5**, 1921 (1972).
[42]R. Pamies, J. G. H. Cifre, and J. G. de La Torre, J. Polym. Sci., Part B: Polym. Phys. **45**, 1 (2007).
[43]R. Pamies, J. G. H. Cifre, and J. G. de La Torre, J. Polym. Sci., Part B: Polym. Phys. **45**, 714 (2007).
[44]P. T. Underhill, "Systematic development of coarse-grained polymer models," Ph.D. dissertation (Department of Chemical Engineering, MIT, Cambridge, MA, 2006).
[45]H. Yamakawa, *Modern Theory of Polymer Solutions* (Harper & Row, New York, 1971).
[46]R. B. Bird, R. C. Armstrong, O. Hassager, and C. F. Curtiss, *Dynamics of Polymeric Liquids* (Wiley, New York, 1987), Vol. 2.
[47]F. Latinwo and C. M. Schroeder, Soft Matter **7**, 7907–7913 (2011).
[48]M.-N. Dessinges, B. Maier, Y. Zhang, M. Peliti, D. Bensimon, and V. Croquette, Phys. Rev. Lett. **89**, 248102 (2002).
[49]J. A. Schellman and D. Stigter, Biopolymers **16**, 1415 (1977).
[50]P. H. von Hippel and O. G. Berg, Proc. Natl. Acad. Sci. U.S.A. **83**, 1608 (1986).
[51]A. Thastrom, P. T. Lowary, and J. Widom, Methods **33**, 33 (2004).
[52]R. M. Elder, T. Emrick, and A. Jayaraman, Biomacromolecules **12**, 3870 (2011).
[53]J. Zebrowski, V. Prasad, W. Zhang, L. M. Walker, and D. A. Weitz, Colloids Surf., A **213**, 189 (2003).
[54]N. Lee and D. Thirumalai, J. Chem. Phys. **113**, 5126 (2000).
[55]A. Kiriy, G. Gorodyska, S. Minko, W. Jaeger, P. Stepanek, and M. Stamm, J. Am. Chem. Soc. **124**, 13454 (2002).
[56]G. Zhang and C. Wu, Phys. Rev. Lett. **86**, 822 (2001).
[57]C. Hyeon, G. Morrison, D. L. Pincus, and D. Thirumalai, Proc. Natl. Acad. Sci. U.S.A. **106**, 20288 (2009).
[58]K. Zhou, Y. Lu, J. Li, L. Shen, G. Zhang, Z. Xie, and C. Wu, Macromolecules **41**, 8927 (2008).
[59]H. K. Murnen, A. R. Khokhlov, P. G. Khalatur, R. A. Segalman, and R. N. Zuckermann, Macromolecules **45**, 5229 (2012).
[60]G. G. Pereira, D. R. M. Williams, and D. H. Napper, Langmuir **15**, 906 (1999).
[61]M. Rubenstein and R. Colby, *Polymer Physics* (Oxford University Press, New York, 2003).
[62]R. K. Pathria, *Statistical Mechanics* (Butterworth-Heinemann, Woburn, MA, 1996).
[63]See supplementary material at http://dx.doi.org/10.1063/1.4917483 for additional formulas used in the computations and simulation data supporting the model used.
[64]A. Montesi, M. Pasquali, and F. C. MacKintosh, Phys. Rev. E **69**, 021916 (2004).
[65]H. P. Babcock, D. E. Smith, J. S. Hur, E. S. G. Shaqfeh, and S. Chu, Phys. Rev. Lett. **85**, 2018 (2000).
[66]I. Saha Dalal, A. Albaugh, N. Hoda, and R. G. Larson, Macromolecules **45**, 9493 (2012).
[67]C. Sendner and R. R. Netz, Eur. Phys. J. E **30**, 75 (2009).